Performance, robustness and noise amplification trade-offs in Disturbance Observer Control design

D. Tena[a], I. Peñarrocha-Alós[a], R. Sanchis[a]

[a] *Departament d'Enginyeria de Sistemes Industrials i Disseny. Universitat Jaume I de Castelló, Spain (e-mail: {david.tenatena,ipenarro,rsanchis}@uji.es).*

Abstract

In this work, we propose a Disturbance Observer (DOB) with a low pass filter with a single tuning parameter. The DOB can be added to a standard PI controller that is assumed to be controlling the system. Our DOB design can be applied to delayed and non-minimum phase systems and is decoupled from the PI control design. We analyse the impact of the DOB filter time constant in disturbance rejection performance, closed loop robustness and measurement noise amplification. The case of First Order plus Time Delay has been studied leading to a set of figures that highlight the trade-offs between those factors and can guide the designer. For arbitrary systems we propose simple rules and instructions for tuning the single parameter of the DOB, taking into account the trade-off between performance, robustness and noise amplification. Finally, we test our proposal experimentally in a real two-tank system setup.

Keywords: Disturbance observer, trade-offs, tuning parameter, non-minumum phase, process control.

1. Introduction

In the scope of process industry, such as chemical, oil and gas or refining, most of the processes run uninterruptedly during long periods of time with the same reference value or setpoint. Furthermore, these processes usually suffer disturbances derived from other processes interaction, weather conditions, sensor noises or faults; so disturbance rejection is the major requisite for controllers. The problem of automatic control is, in essence, that of disturbance rejection [1].

Feedback controllers, specifically PI and PID controllers, are the most common regulatory control algorithms in process industry [2]. When using a feedback controller, disturbance rejection can be addressed in several ways [3, 4].

Without adding any new element to the control structure, a passive strategy consists of selecting the proper controller tuning for disturbance rejection. In that sense, [5] and [6] propose tuning rules that improve disturbance response; [7] exposes a robust design for PI synthesis; [8] presents a pole placement technique that consists of avoiding *plateaus* in frequency response from disturbance to output, and [9]proposes an optimal PI tuning through genetic algorithms. Furthermore, [10] proves that a PI itself can act like a controller plus and observer in certain kind of systems. If disturbances are measurable, a feed-forward action can be added to directly correct its effect. The main design rules can be reviewed in the recent works [11, 12].

On the other hand, an active strategy incorporates some extra elements in the control structure whose task is to estimate or observe the disturbance and, then, to feed-forward the necessary control action for cancelling the disturbance effect. The authors in [13] review different observers proposed over the years regarding its complexity, dynamical structure, information required and implementation, while in the recent work [14], the authors compare the observer based techniques among others. Active Disturbance Rejection Control (ADRC) has emerged as a popular technique since the end of the 90's decade as an alternative to feedback control [15, 16, 17, 18]. It is a state feedback control that uses an Extended State Observer (ESO) to estimate the disturbance. Some applications in power plants and chemical processes can be found in [19, 20, 21, 22, 23]. This technique can also be applied to multivariable processes [24, 25, 26] or systems with unstable or non-invertible dynamics [27, 28].

Other state space observer solutions are found in [29], where the disturbance signal is changed by an equivalent input disturbance (EID) in order to simplify the control structure; in [30], the state estimation is performed by a new set of filters; in [31], a tuning approach based on bounded system norms is proposed; in [32], the technique is extended to non-linear systems and, more recently, in [33] and [34]. Other recent works are [35], where a FIR architecture is used to estimate future states based on previous observations, or [36], where a disturbance estimation iis used in a predictive controller.

The main disadvantage of ADRC is that its design through a state observer requires complex algebraic operations that require high control engineering knowledge, and we consider that a handicap to become a mainstream solution in industrial applications. On the contrary, the success of standard feedback control structures like PI derives from the ease of use, due to the few tuning parameters

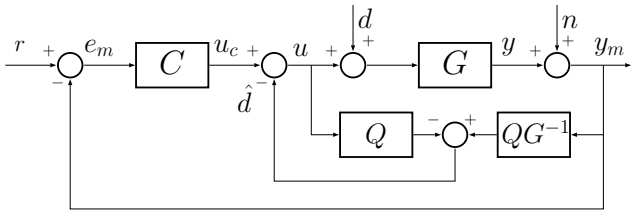

Figure 1: DOB control structure.

and the existence of standard implementation functions in control devices (as Programmable Logic Controllers or Distributed Control Systems).

Another solution is a Disturbance observer (DOB), that is an additive structure whose aim is to estimate the disturbance and feed it forward to improve a standard feedback control (see figure 1). It is thought to be implemented in an input-output procedure and its design consists of inverting the process input-output transfer function model to estimate the disturbance. To ensure a proper observer, a filter (Q in the figure) is added so that the relative degree of the inverted plant transfer function is not negative. DOB is the base for the control structure proposed in this work.

The design of the filter Q plays a main role in disturbance rejection performance as well as in closed loop robustness and measurement noise amplification. Many references can be found in the literature about DOB control. However, from our point of view, they have some drawbacks that we try to tackle, to ensure that it can be applied to any kind of industrial process and that the design is straightforward enough to encourage every worker in industry, not only control systems specialists, to use it.

When inverting the plant model, elements like time delays and half-right zeros make the model inverse unstable or non-realizable. In [37], model inversion is not contemplated. In [38, 39], authors do not include in the process these above mentioned elements. [40] presents a novel control structure equivalent to a PI plus DOB but with only a PI and a reference filter, but it is restricted to minimum-phase systems. [41] presents a method that is suitable for non-minimum-phase systems based in a filter in parallel with the plant that makes the global set minimum-phase, but this solution adds complexity to the DOB structure.

Some applications of DOB control can be found in [42, 43, 44, 45, 46], as a dual process simulator, a stirred tank process, a heating system, a refrigeration system and a ball balancer. In all of them, the design of the time constant of the filter Q is chosen heuristically, with the only concern of being small enough to guarantee an improvement on disturbance rejection, or tuned in a trial and error method, checking the results after.

The computation of optimal solutions regarding system norms is the approach proposed in [47, 48, 49, 50, 51]. Although this strategy is more rigorous, it requires the use of complex computer techniques to optimize system standards, distancing them from the day-to-day operation of an industrial plant by plant operators and engineers with less control theory knowledge. This also happens with adaptive DOB proposals, as [52] and [53], based in *ad hoc* solutions more difficult to extend to other systems.

Another important aspect to consider is that, when we feed back a signal from the process output, we introduce the sensor measurement noise in the loop, affecting the actuator behaviour. Closed-loop control has this drawback, and the inclusion of the DOB worsens this situation. In [54] and [55], the authors consider a trade-off between disturbance rejection performance and robustness by starting with a relatively fast filter and then slowing it to achieve smoothness, but noise amplification is not considered. [56] and [57] do not consider noise effect for the filter tuning either. On the contrary, [58] considers noise effect in the design of the filter and deals with the elements of the process model whose inverse lead to an unstable or non-realizable system. However, it does not consider closed loop robustness. These control structures are aimed to improve the behaviour under disturbances, but its presence affects also to the amplification from measurement noise to actuator activity and to the final closed-loop robustness, that differs from standard feed-back control. Other references that refer to this trade-off are [59, 60, 61, 62, 63].

Considering this state of the art, in this work we propose a DOB control structure that is added to a standard PI control, with the following features:

- The DOB requires a model of the plant and includes a low pass filter with a single tuning parameter.
- We provide simple tuning rules for this single tuning parameter that take into account the trade-offs between three indicators: disturbance rejection performance, closed-loop robustness and impact of noise in the control action activity. Trade-off plots are also provided to help the designer to achieve a given trade-off for simple widely used models.
- It is suitable for non-minimum-phase systems, and processes with time delay.
- The DOB design is decoupled from the PI controller design and we quantify the new behaviour performance with our DOB in relative terms w.r.t the original behaviour with just a PI controller. There is no need to modify the existing PI controller to improve disturbance rejection with our proposal.

As we will see later, low values of the filter time constant lead to better disturbance rejection but poorer robustness and more noise amplification from sensor to actuator. This study is inspired in [64], which shows a similar trade-off behaviour in PI control. In this work, our approach is not to find the best estimation of the disturbance but to find the best signal to feed forward in order to fulfil some requirements in terms of these three indicators.

The authors have previously studied disturbance estimation in the work [65], but no feed-forward was included in the analysis, which is only focused on optimal disturbance estimation.

We show that this trade-off depends also on the process dynamics. In particular, we analyse this dependency with the normalized time delay for FOTD systems (normalized time delay is in the range between 0 and 1). We present trade-off plots that can be used for tuning purposes for FOTD systems, starting from the process dynamics and the targets on performance, robustness and noise amplification.

The article is structured as follows. Section 2 exposes the problem statement and the objectives of the work. In Section 3 we explain the disturbance observer (DOB) structure. Section 4 shows some examples on simulated plants, comparing the performance between them, while in section 5 we present the trade-off plots and a test in a batch of process models commonly used in literature. Section 6 gives the tuning guidelines and some implementation instructions for practitioners. Section 7 includes an experimental example in a real two-tank system recreated in the laboratory. Finally we report the conclusions on section 8.

2. Problem Statement

Let us consider a LTI process $G(s)$ with an input $u(s)$, an output $y(s)$, and affected by a non measured input disturbance $d(s)$.

$$y(s) = G(s)(u(s) + d(s)). \tag{1}$$

The measured output $y_m(s)$ contains a noise signal $n(s)$, so that

$$y_m(s) = y(s) + n(s). \tag{2}$$

A feedback controller computes the control action $u_c(s)$ as

$$u_c(s) = C(s)e(s),\ e(s) = r(s) - y_m(s), \tag{3}$$

where $r(s)$ is the reference signal, $C(s)$ is the controller transfer function and $e(s)$, the measured tracking error.

In this work we consider that the controller is a PI control defined as

$$u_c(t) = K_p \left(e(t) + \frac{1}{T_i} \int_0^t e(\tau) d\tau \right), \tag{4}$$

$$\frac{u_c(s)}{e(s)} = C(s) = K_p \left(1 + \frac{1}{T_i\, s} \right) = K_p + \frac{K_i}{s} \tag{5}$$

where K_p is the proportional gain, T_i the integral time and $K_i = \frac{K_p}{T_i}$ the integral gain. We assume that the controller is previously tuned and implemented through standard functions that include anti-windup, bumpless transfer and offset options, i.e., is implemented through the periodical computation (each T_s seconds) of the following equations

$$e = r - y_m \tag{6}$$

$$I = I + T_s\, e \tag{7}$$

$$u_c = K_p\, e + K_i\, I \tag{8}$$

$$u = saturate(u_c + u_f) \tag{9}$$

$$I = \begin{cases} I & if\ u = u_c + u_f \\ I + AW & otherwise \end{cases} \tag{10}$$

where the signals refer to their value at the sampling instant, I is the integral term of the tracking error, u_c refers to the pure PI computation, u_f refers to the offset value, and u refers to the finally applied control action. The term AW refers to any applicable anti-windup or bumpless transfer technique (as $AW = -T_s\, e$ or $AW = K_t(u - u_c - u_f)$, with K_t the anti-windup gain, see [66, 67]). The function "saturate" indicates that we apply the minimum or maximum available value for u if $u_c + u_f$ is out of those bounds.

We assume in this work that we have a PI control running on the system that has available an offset signal to apply any convenient value. This can be used, for instance to help initializations, or to apply feed-forward control from measured disturbances. This is a common situation in industry. In this work we will propose to use that signal u_f to improve the behaviour under disturbances through the use of a disturbance observer. We assume that the controller has been already tuned and is working on the plant. This work assumes a PI controller, but the study for PID control can be easily extended, and the general results are still valid.

When we do not have any offset signal, the system input is thus given by the control action, $u(s) = u_c(s)$ and behaves in closed loop as

$$u(s) = \frac{C(s)r(s) - G(s)C(s)d(s) - C(s)n(s)}{1 + G(s)C(s)}. \tag{11}$$

$$e(s) = \frac{r(s) - G(s)d(s) + G(s)C(s)n(s)}{1 + G(s)C(s)}. \tag{12}$$

With the assumed PI controller with $C(s) = K_p + \frac{K_i}{s}$, we can state that the controlled process has the following performance indices w.r.t. robustness, reference tracking, disturbance rejection, and noise effect on the control action. For further comparisons, we define the following indicators regarding each index:

A. Performance versus reference

A1. Steady state error under step reference.

$$\lim_{s \to 0} \frac{1}{1 + G(s)C(s)} = 0$$

A2. Integral error (IE) under step reference.

$$\lim_{s \to 0} \frac{1}{1 + G(s)C(s)} \frac{1}{s} = \frac{1}{K_i G(0)}$$

B. Performance versus disturbance

B1. Steady state error under step disturbance.

$$\lim_{s\to 0} \frac{-G(s)}{1+G(s)C(s)} = 0$$

B2. Integral error (IE) under step disturbance.

$$\left| \lim_{s\to 0} \frac{-G(s)}{1+G(s)C(s)} \frac{1}{s} \right| = \frac{1}{K_i}$$

B3. Integral error (IE) under ramp disturbance.

$$\lim_{s\to 0} \frac{C(s)}{1+G(s)C(s)} \frac{1}{s^2} = \infty$$

C. Robustness: Maximum peak of the sensitivity function $S(s)$ given by $M_s = \max_\omega |S(j\omega)|$, where $S(s)$ is defined as ([68])

$$S(s) = \frac{dT(s)/T(s)}{dG(s)/G(s)}, \qquad T(s) = \frac{y(s)}{r(s)}. \tag{13}$$

From (1) and (11),

$$T_0(s) = \frac{C(s)G(s)}{1+C(s)G(s)}, \tag{14}$$

$$S_0(s) = \frac{1}{1+C(s)G(s)}, \tag{15}$$

$$M_{s,0} = \max_\omega |S_0(j\omega)|. \tag{16}$$

Note that we denote with subindex 0 the original values with a PI control (before adding our proposal).

D. Noise effect: direct gain from the sensor noise $n(s)$ to the control action $u(s)$ (assuming high frequency noises):

$$A_{n,0} = \left| \lim_{s\to\infty} \frac{-C(s)}{1+G(s)C(s)} \right| = C(\infty) = K_p,$$

that can also be seen as a measure of the control effort.

The objectives of this paper are:

- To develop a disturbance observer (DOB) to improve disturbance rejection, as an additive structure for a PI controller that has been already designed and implemented.
- To offer easy tuning and implementation rules based in previous indicators.
- To develop trade-off plots that show the relationship between robustness, disturbance rejection and actuator activity due to measurement noise as a guide for the designer.

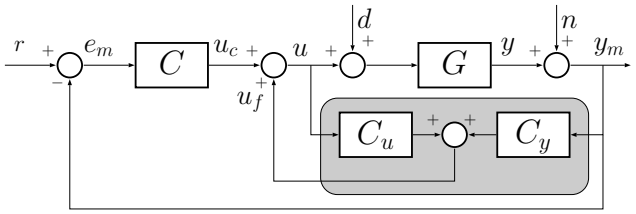

Figure 2: Proposed control scheme. DOB, composed by C_u and C_y, is shadowed in gray.

The improvement in disturbance rejection is understood as the kind of disturbance signals that the new controller can cancel, we do not refer to improving the disturbance behaviour for the same kind of disturbances or to speeding up the controller for reference tracking, that would be a task for the PI designer. Our proposal tries to take profit of the offset signal generally available in standard PI control and the integrated saturation and anti-windup mechanism.

3. Disturbance Observer structure

In this section, we explain the proposed Disturbance Observer (DOB) and we describe the steps followed to end up with its particular structure. The control action $u(s)$, which is the input of the process, consists of two terms,

$$u(s) = u_c(s) + u_f(s), \tag{17}$$

being $u_c(s)$ the pure PI controller output and $u_f(s)$, the DOB output that we feed-forward and that can be implemented through the offset term in standard PI implementation.

The proposed DOB inputs are the resulting process input u (after PI, DOB and saturation operation) and the measured output y_m. The DOB output, $u_f(s)$, is defined by

$$u_f(s) = C_u(s)u(s) + C_y(s)y_m(s), \tag{18}$$

being $C_u(s)$ and $C_y(s)$ two transfer functions detailed later. Ideally, we would like to feed-forward the current disturbance signal for perfect disturbance rejection. However, this is not measured and it can only be estimated. Perfect estimation requires to invert G, which results in a non-proper transfer function. Estimation approaches can also lead to potential model errors that can compromise the performance and robustness of the controller. Our approach is not to find the best estimation of the disturbance but to find the best signal to feed-forward in order to fulfil some requirements in terms of controller performance against disturbances, robustness and noise effect.

Figure 2 shows the complete control scheme proposed, where we can see the integration of the PI controller C and the DOB, which consists of C_u and C_y[1].

[1] One must understand that after the summation node $u_c + u_f$ there would be the saturation function, that would also affect the integral term in the C block. The figure only indicates the linear behaviour for stability analysis.

If we define the characteristic polynomial of the closed loop as

$$D(s) = 1 + G(s)C(s) - C_u(s) - G(s)C_y(s), \quad (19)$$

the tracking error and control action response are given by

$$\begin{aligned} u(s) &= \frac{1}{D(s)}\left[C(s)r(s)\right. \\ &\quad -G(s)(C(s)-C_y(s))d(s) \\ &\quad \left.-(C(s)-C_y(s))n(s)\right], \quad (20) \\ e(s) &= \frac{1}{D(s)}\left[(1-C_u(s)-C_y(s)G(s))r(s)\right. \\ &\quad -G(s)(1-C_u(s))d(s) \\ &\quad \left.+G(s)(C(s)-C_y(s))n(s)\right]. \quad (21) \end{aligned}$$

where $e = r - y$ is the tracking error (and not the measured error e_m).

3.1. Objectives and requirements

We look for the DOB to fulfill the next objectives related with previous section indicators:

A. To keep performance versus reference.

A1. To keep the steady state error under step reference at zero,

$$\lim_{s\to 0} \frac{1 - C_u(s) - C_y(s)G(s)}{D(s)} = 0,$$

A2. To keep the Integral error (IE) under step reference,

$$\lim_{s\to 0} \frac{1 - C_u(s) - C_y(s)G(s)}{D(s)} \frac{1}{s} = \frac{1}{K_i G(0)},$$

B. To improve performance versus disturbances (step and ramp-like).

B1. To keep steady state error under step disturbances at zero,

$$\lim_{s\to 0} \frac{-G(s)(1 - C_u(s))}{D(s)} = 0,$$

B2. To improve the Integral error (IE) under step disturbances,

$$\left|\lim_{s\to 0} \frac{-G(s)(1 - C_u(s))}{D(s)} \frac{1}{s}\right| \leq \frac{1}{K_i}.$$

B3. To improve the Integral error (IE) under ramp disturbances,

$$\left|\lim_{s\to 0} \frac{-G(s)(1 - C_u(s))}{D(s)} \frac{1}{s^2}\right| < \infty.$$

C. To ensure a certain degree of robustness,

$$M_s < \gamma_1.$$

D. To ensure a certain noise amplification limitation from sensor noise to control action,

$$A_n = \left|\lim_{s\to\infty} \frac{-C(s) + C_y(s)}{D(s)}\right| < \gamma_2.$$

This may be interpreted as a performance measure of the impact of noise on actuator activity (this could be also addressed through other similar indices as the Total Variation [69]).

Besides, we require stable and realizable transfer functions, so C_u and C_y must be causal.

3.2. Structure proposal

Let us consider the process transfer function in the form

$$G(s) = \frac{K \prod_{i=1}^{m}(1+\beta_i s) \prod_{i=1}^{n}(1-\delta_i s)e^{-Ts}}{s^k \prod_{i=1}^{p}(1+\tau_i s)}, \quad (22)$$

where $k = 1$ if the system has an integrator and $k = 0$ if not, and where β_i, $\delta_i > 0$. K stands for the static gain (without the integrator, in that case), $-1/\beta_i$ are the half-left zeros in the complex plane and $1/\delta_i$, the half-right ones. T is the time delay of the system, and $-1/\tau_i$ are the poles in $G(s)$, both stable and unstable. If the system has complex poles, one must interpret that there would be a couple of conjugate values in τ_i. Let us now express the transfer function as

$$G(s) = K\, G_I(s) G_N(s), \quad (23)$$

where

$$G_I(s) = \frac{\prod_{i=1}^{m}(1+\beta_i s)}{s^k \prod_{i=1}^{p}(1+\tau_i s)}, \quad (24)$$

$$G_N(s) = \prod_{i=1}^{n}(1-\delta_i s)e^{-Ts}, \quad (25)$$

in order to conveniently consider the terms whose inverse leads to a stable system ($G_I(s)$) and the terms which not ($G_N(s)$). $G_N(s)$ also includes the delay, as one cannot implement its inverse. With the aim of simplicity in design and implementation, we propose then

$$C_u(s) = \frac{G_N(s)}{(1+\alpha\, s)^d}, \quad (26)$$

$$C_y(s) = \frac{-G_I^{-1}(s)}{K(1+\alpha\, s)^d}, \quad (27)$$

where α is the tuning parameter and where $d = p + k - m$ is the relative degree of $G_I(s)$. By including the filter terms $(1+\alpha\, s)^d$ in the denominator we ensure that $C_y(s)$ is proper. Assuming that the transfer function $G(s)$ is strictly proper (as usually in real systems), $d > 0$. Then, the relative degree of $C_u(s)$ is positive and thus $C_u(s)$ is proper too. Note that the proposed structure fulfills

$$C_u(s) + C_y(s)G(s) = 0, \quad (28)$$

which, considering (19), implies

$$D(s) = 1 + G(s)C(s), \tag{29}$$

i.e., the characteristic polynomial of the closed loop (19) is not altered w.r.t. the original one shown in (11) and (12) and, therefore, the stability of the closed-loop system with our proposal is guaranteed.

The filtering term $(1+\alpha\, s)^d$ in (26) and (27) could also be chosen, generally, as any stable polynomial of order d. This would lead to more degrees of freedom in the design that can also lead to better performance. However, in this work, we focus on simplicity both on design and implementation that ease the use of this technique and, thus, we determine design laws with just one tuning parameter.

3.3. Structure properties

The choice of the proposed structure fulfils the next properties regarding above mentioned indicators:

A. Applying equation (21), with equations (22) to (27), we see that

$$\frac{e(s)}{r(s)} = \frac{1}{1 + G(s)C(s)}, \tag{30}$$

which coincides with the transfer function in the original PI control. Therefore,

$$T(s) = \frac{y(s)}{r(s)} = \frac{C(s)G(s)}{1 + G(s)C(s)} = T_0(s), \tag{31}$$

so we keep the reference tracking behavior, i.e., indicators A1 and A2.

B. B1. We keep null steady state error under step disturbance.

B2. From (20), we prove that the IE under step disturbances in absolute value now is zero, i.e.,

$$\left| \lim_{s\to 0} s \frac{-G(s)\left(1 - \frac{G_N(s)}{(1+\alpha\, s)^d}\right)}{1 + G(s)C(s)} \frac{1}{s} \right| = 0. \tag{32}$$

Since the static gain of the transfer function $G_N(s)$ is unitary (i.e., $G_N(0) = 1$), the previous limit is zero. This implies that we will obtain oscillatory behaviour under step disturbances. This is one of the implications of having two mechanisms for the rejection of disturbances (the integral term of the PI control plus the DOB term).

B3. Previous indicator also implies the ability to reject ramp disturbances in steady state, unlike the original feedback controller. This is one of the main advantages of having two mechanisms for disturbance rejection. The integral error under ramp disturbances is now finite and is given by

$$\left| \lim_{s\to 0} s \frac{-G(s)\left(1 - \frac{G_N(s)}{(1+\alpha\, s)^d}\right)}{1 + G(s)C(s)} \frac{1}{s^2} \right| = \frac{d\,\alpha + T + \sum \delta_i}{K_i}, \tag{33}$$

being d the relative degree of $G_I(s)$. The performance in rejecting ramp disturbances depends on the tuning parameter α as well as the process dynamics and the PI controller gain K_i (assumed to be previously tuned depending on the process model or through experimental procedures).

C. The sensitivity function of the whole control structure including the DOB, considering (13) and (28), becomes

$$S(s) = \frac{1 - C_u(s)}{1 + C(s)G(s)} = S_0(s)(1 - C_u(s)). \tag{34}$$

The resulting sensitivity function differs from the one in the original PI control structure since the numerator includes the term $1 - C_u(s)$. According with (26), the sensitivity function will depend on the non-invertible terms of $G(s)$, which are the time delay T, and the half-right zeros in the complex plane δ_i. We can state that the sensitivity peak fulfils

$$M_s = \max_{\omega} |S(j\omega)| \leq M_{s,0} \cdot \max_{\omega} |1 - C_u(j\omega)|\,, \tag{35}$$

and, therefore, $(1-C_u(s))$ is the term that can worsen the new robustness. We will see later that robustness with DOB worsens more for long time delays.

D. Due to the feed-forward of a signal which depends on measurement noise, the noise effect in the control action gets higher. The amplification for high frequency noises is now given by

$$A_n = \left| \lim_{s\to\infty} \frac{-C(s) - \frac{G_I^{-1}(s)}{(1+\alpha\, s)^d}}{1 + G(s)C(s)} \right| = K_p + \frac{\prod \tau_i}{\prod \beta_i\, \alpha^d}. \tag{36}$$

Therefore, the noise amplification depends on the tuning parameter α as well as on the process dynamics and PI tuning.

3.4. Proposal summary

In summary, we propose a Disturbance Observer (DOB), which can be added to a currently installed and configured feedback controller, composed of two transfer functions,

$$C_u(s) = \frac{G_N(s)}{(1 + \alpha\, s)^d}, \quad C_y(s) = \frac{-G_I^{-1}(s)}{K(1 + \alpha\, s)^d}.$$

The properties of this structure are:

A. Closed loop reference tracking behaviour is not modified w.r.t. PI control when we incorporate the DOB to the control structure.

B. DOB modifies the performance on disturbance rejection. It cancels the IE under step disturbances, but we will obtain oscillatory responses. It allows us to reject ramp disturbances in steady state, and the behaviour depends on the tuning parameter α.

C. It has a negative impact on closed-loop robustness, which also depends on the tuning parameter α.

D. It also has a negative impact on measurement noise amplification and, again, this depends on the tuning parameter α.

Disturbance rejection performance improves as α decreases, but robustness and noise amplification worsens if α decreases. Therefore, the tuning of α implies a trade-off between these indicators. We have also shown how the impact of the proposed DOB in the closed-loop performance against disturbances, robustness, and noise amplification does not only depend on the tuning parameter α but it also depends on the current process dynamics (see (33)).

In the next section, we will illustrate this through some examples.

4. Numerical FOTD examples

In this section we detail the behavior of the proposed DOB with different numerical examples in First Order plus Time Delay (FOTD) systems,

$$G(s) = \frac{K}{1+\tau\, s} e^{-Ts}. \tag{37}$$

This allows us to simplify the process dynamics considerations by using the normalized time delay, which is the time delay divided by the sum of the lag and the time delay, i.e., $\frac{T}{T+\tau}$, and which is in the range between 0 and 1.

According to (26) and (27), the DOB in case of FOTD processes reduces to

$$C_u(s) = \frac{e^{-Ts}}{(1+\alpha\, s)}, \tag{38}$$

$$C_y(s) = -\frac{1+\tau\, s}{K(1+\alpha\, s)}. \tag{39}$$

4.1. Implications of the DOB

We can obtain for this FOTD which is the implication of using DOB. In the one hand we have the benefit of including it to improve disturbance rejection against ramps and, for lower values of α, we also have better step disturbance rejection. On the other hand, we have that including the DOB may worsen the robustness as indicated in (35) and may amplify the measurement noise by adding a term τ/α (see (36)). Figure 3 shows the values of the effect on robustness and noise amplification as a function of α and the normalized time delay. We see that the robustness worsening is negligible (i.e. the values of $|1 - C_u(j\omega)|_\infty$ are near 1) when using high values of α or if the delay is low, and the noise amplification increment is low (i.e. τ/α is low) if α is high or the delay is high. In order to better understand this trade-offs, in the next subsection we combine these results with the use of the PI controller that is adequate for each process.

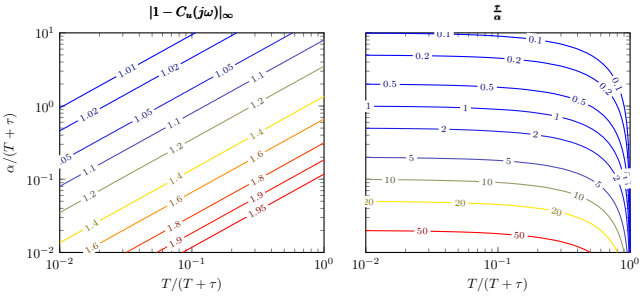

Figure 3: Trade-off plots. Bound on relative robustness and noise amplification.

4.2. Batch of plants and controllers

We consider three plants with normalized time delays of 0.05, 0.2 and 0.9, which is the time delay divided by the sum of the lag and the time delay. For easing the comparison, all the plants simulated fulfill $(T+\tau) = 100$.

We have tested also two different PI controllers for each plant: one tuned with an initial sensitivity peak $M_{s,0} = 1.2$, which is a robust and conservative value typically used in industrial applications where robustness is a main requisite, and another one with $M_{s,0} = 2$, which is an aggressive but still reasonable value. For comparison reasons, the PI controllers have been tuned with the following rule

$$\max K_i \qquad \text{subject to}: M_{s,0} = M_{s,d}$$

being $M_{s,0}$ the sensitivity peak with the PI controller, and $M_{s,d}$ the desired value. With this in mind, the controller is the one that minimizes the IE under step disturbance, and the one that minimizes the steady state error under ramp disturbances.

For each of the mentioned plants and PI controllers combination, we have simulated the response with and without the DOB proposed in the paper, considering a value for α that is 100%, 10% and 1% of the process $(T+\tau)$.

Tables 1 and 2 summarize the different scenarios tested in this section, where K_p is the proportional gain and T_i the integral time of the PI controller, as defined in (4).

Table 1: Numerical examples, PI with $M_{s,0}$=1.2

Plant	$G(s)$	K_p	T_i	DOB tuning
1	$\frac{1}{1+95s}e^{-5s}$	3.3	35.2	No DOB,
2	$\frac{1}{1+80s}e^{-20s}$	0.71	57.9	$\alpha = 100$,
3	$\frac{1}{1+10s}e^{-90s}$	0.13	48.9	$\alpha = 10$,
				$\alpha = 1$.

Table 2: Numerical examples, PI with $M_{s,0}$=2.

Plant	$G(s)$	K_p	T_i
1	$\frac{1}{1+95s}e^{-5s}$	11	19.9
2	$\frac{1}{1+80s}e^{-20s}$	2.16	41
3	$\frac{1}{1+10s}e^{-90s}$	0.31	36.1

DOB tuning
No DOB,
$\alpha = 100$,
$\alpha = 10$,
$\alpha = 1$.

To analyse the performance achieved in each case, we consider the indicators mentioned throughout the work. Since the behaviour under references remains unaltered (indicator A) and since the IE under step disturbances (indicator B2) has been proven to be null, we use a different set of indicators on step disturbance rejection. The complete list of indicators is then the following:

B2-I. Integral of Absolute Error (IAE) versus step disturbances,

$$IAE = \lim_{t\to\infty} \int_0^t |e_m(\tau)| d\tau.$$

B2-II. Integral of Squared Error (ISE) versus step disturbances,

$$ISE = \lim_{t\to\infty} \int_0^t e_m^2(\tau) d\tau.$$

B2-III. Integral of Time-weighted Absolute Error ($ITAE$) versus step disturbances,

$$ITAE = \lim_{t\to\infty} \int_0^t \tau\ |e_m(\tau)| d\tau.$$

B2-IV. Maximum absolute value of the error versus step disturbances,

$$e_{\max} = \max_t |e_m(t)|. \tag{40}$$

B2-V. Total variation of the control action versus step disturbances,

$$TV = \lim_{t\to\infty} \int_0^t \left| \frac{du(\tau)}{d\tau} \right| d\tau. \tag{41}$$

B3. Integral Error (IE) under ramp disturbances,

$$IE = \frac{\alpha + T}{K_i}$$

C. Sensitivity Peak (M_s),

$$M_s = \max_\omega S(j\omega), \tag{42}$$

where $S(s)$ is the sensitivity function (34).

D. High-frequency noise amplification (A_n), which considering (36) becomes

$$A_n = K_p + \frac{\tau}{\alpha}. \tag{43}$$

4.3. Disturbance rejection

Figure 4 shows the time response of the measured tracking error $e(s)$ under step and ramp disturbances $d(s)$. We have simulated a unitary step disturbance followed by a 0.01 slope ramp disturbance. In processes with low time delay, the improvement that we can achieve using DOB control w.r.t. standard PI control is higher than in processes with high time delay. This effect is even more noticeable with low values in α. Moreover, as the time delay becomes more significant, the error response presents a big overshoot, which can be undesirable. We can also notice that, if the PI controller has a more conservative tuning (designed with a lower sensitivity peak $M_{s,0}$) and we include the proposed DOB, we achieve better results in performance indicators. However, if the PI controller has an aggressive tuning and the time delay is high, by adding our DOB we can even worsen the disturbance rejection behaviour when reducing α (see Plant 3 for $M_{s,0} = 2$). This is the case where we have to be careful using the DOB. In tables 3 and 4, we can check the numerical results for the considered indices under step disturbance. IAE_0, ISE_0, $ITAE_0$, $e_{\max,0}$ and TV_0 refer to the indices obtained using only the PI controller (without the DOB), while IAE, ISE, $ITAE$, $e_{\max}$ and TV refer to those obtained when we add the DOB. We show the ratios between them in the tables, so a value lower than 1 means that we have improved the result and a value higher than 1 means that we have worsen it. We can also see how, by including the DOB, we are able to reject ramp disturbances and this rejection is better for lower values of α (see (33)).

Figure 6 shows the frequency response of the tracking error $e(s)$ due to disturbance $d(s)$. In Plant 1 (low time delay), the DOB reduces the magnitude in the whole frequency spectrum as the value of α decreases. As long as the time delay increases (in Plant 2 and specially in Plant 3), disturbance rejection is still better in low frequencies for low values of α (lower magnitude in the figure) but the response for higher frequencies gets worse, so the use of lower values of α is less appropriate. This effect is more pronounced if the PI controller has a more aggressive tuning (higher $M_{s,0}$).

4.4. Robustness

Figure 7 shows the frequency response of the sensitivity function $S(s)$, as defined in (16) and (34) for the cases with and without the DOB. The sensitivity peak M_s, which indicates the robustness of the closed loop, is the maximum of this function; we have marked it in the figure. Generally, including DOB increases M_s w.r.t. to using only PI control. We cannot assume a strictly increasing dependency between α and M_s (see cases with $M_{s,0} = 2$ in figure 7).

4.5. Noise amplification

Figure 8 shows the frequency response of the control action $u(s)$ due to the measurement noise $n(s)$. In the three plants, independently of the process time delay, the

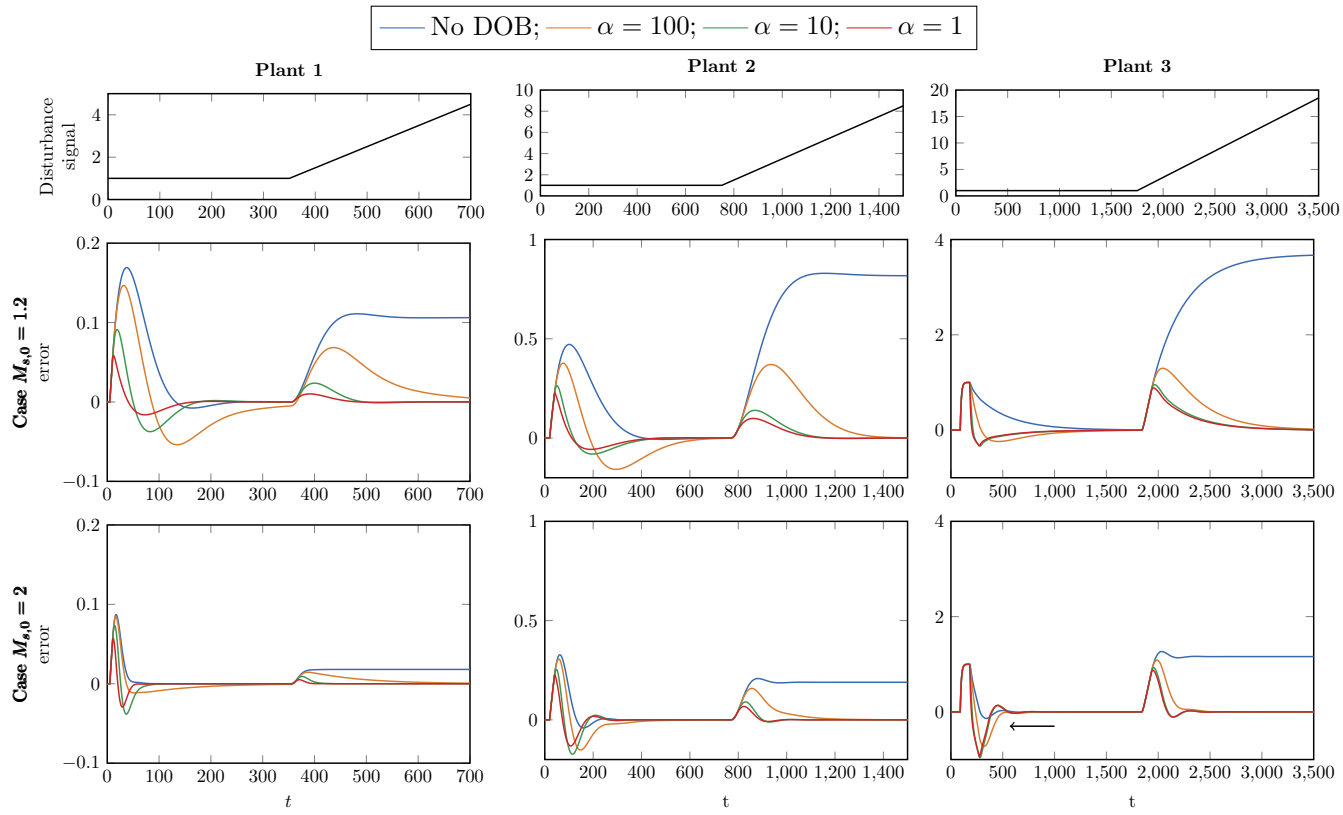

Figure 4: Numerical example. Disturbance to step plus ramp error time response.

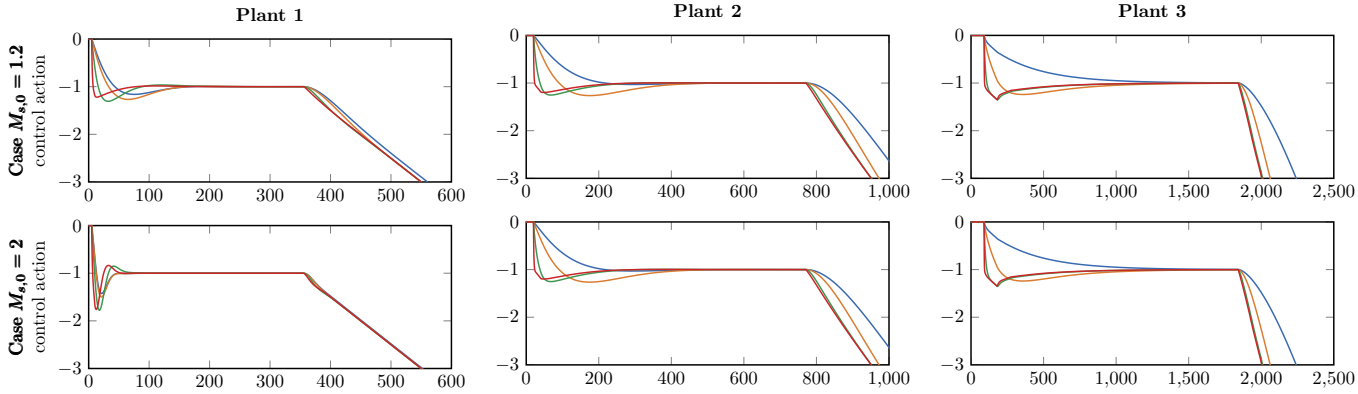

Figure 5: Numerical example. Control action time response under step plus ramp disturbance.

high frequency noise amplification increases as we reduce the value of α (noise amplification is less pronounced if the time delay is higher). For systems with higher time delay, the frequency response presents wrinkles, which means that the noise amplification is lower for certain particular frequencies. The increase in noise amplification as a function of α is similar for all the plants and controllers, but the absolute value of noise amplification depends on the proportional gain of the considered PI controller, that defines the noise amplification for the case without DOB, see (36) and (43).

Table 3: Numerical examples results $M_{s,0} = 1.2$

$\frac{T}{T+\tau}$	$\frac{\alpha}{T+\tau}$	$\frac{IAE}{IAE_0}$	$\frac{ISE}{ISE_0}$	$\frac{ITAE}{ITAE_0}$	$\frac{e_{\max}}{e_{\max,0}}$	$\frac{A_n}{A_{n,0}}$	$\frac{TV}{TV_0}$
	1	1.2	0.727	2.426	0.86	1.3	1.16
0.05	0.1	0.41	0.155	0.46	0.526	4	1.26
	0.01	0.174	0.035	0.173	0.335	31	1.09
	1	0.856	0.504	1.27	0.8	2.135	1.44
0.2	0.1	0.321	0.117	0.327	0.555	12.35	1.43
	0.01	0.227	0.064	0.222	0.477	114.5	1.32
	1	0.728	0.62	0.78	1	1.99	1.47
0.9	0.1	0.527	0.475	0.443	1	10.89	1.69
	0.01	0.488	0.44	0.401	1	100	1.69

Table 4: Numerical examples results $M_{s,0} = 2$

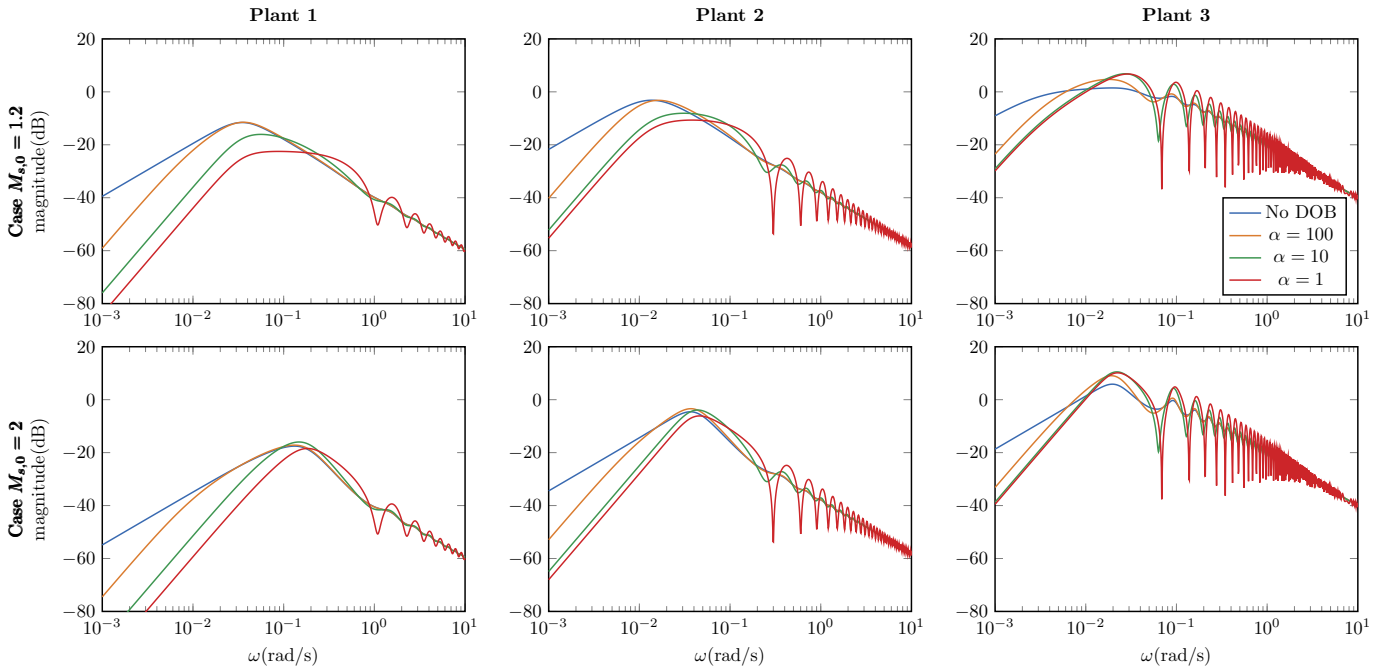

Figure 6: Numerical example. Disturbance to error frequency response.

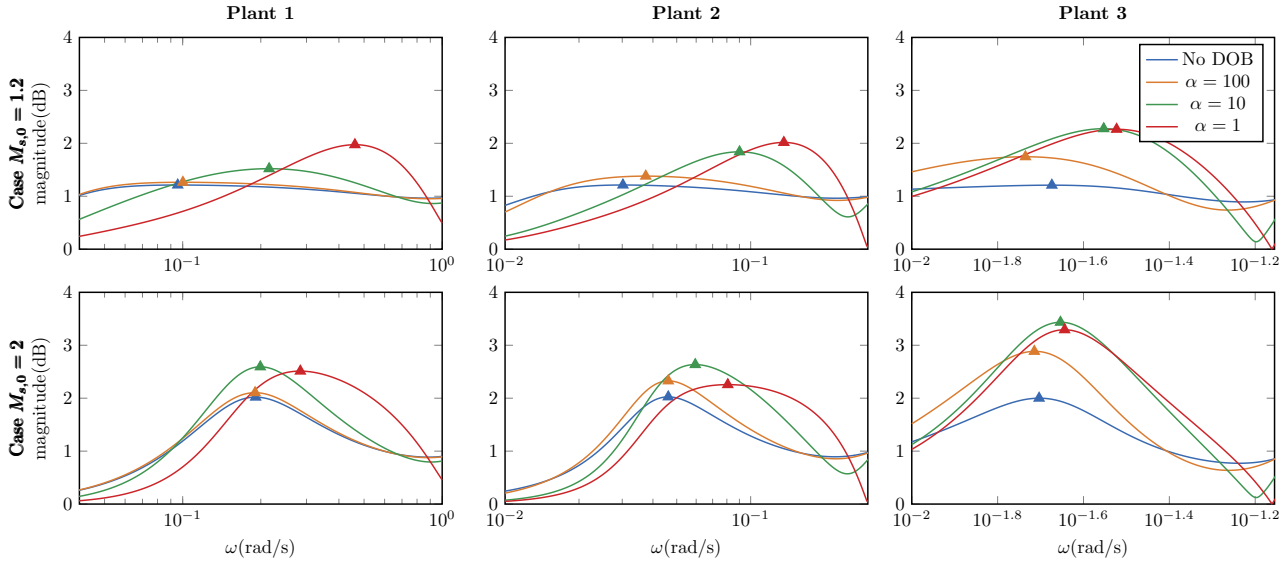

Figure 7: Numerical example. Sensitivity function frequency response (M_s, i.e. function maximum, marked)

$\frac{T}{T+\tau}$	$\frac{\alpha}{T+\tau}$	$\frac{IAE}{IAE_0}$	$\frac{ISE}{ISE_0}$	$\frac{ITAE}{ITAE_0}$	$\frac{e_{\max}}{e_{\max,0}}$	$\frac{A_n}{A_{n,0}}$	$\frac{TV}{TV_0}$
	1	1.573	0.983	4.71	0.968	1.1	1.08
0.05	0.1	1.02	0.737	1.29	0.819	2.02	1.53
	0.01	0.588	0.293	0.656	0.6256	11.17	1.54
	1	1.361	0.996	1.99	0.931	1.4	1.28
0.2	0.1	0.861	0.576	1.03	0.768	4.95	1.65
	0.01	0.642	0.345	0.724	0.681	40.5	1.44
	1	1.51	1.42	1.99	1	1.33	1.86
0.9	0.1	1.48	1.48	1.87	1	4.29	2.50
	0.01	1.4	1.36	1.73	1	33.9	2.5

Finally, we test in plant 1 with the PI controller designed with $M_{s,0} = 1.2$ the use of the DOB when the disturbance is a random walk, to show the effectiveness in more realistic scenarios. We show in figure 9 the disturbance signal, the output and the control action when controlling only with the PI, and when adding the DOB. We show in table 5 performance indices IAE, ISE, $ITAE$, $e_{\max}$ and TV in relative terms w.r.t. to standard PI control, showing the improvement with the proposed approach at the cost of some increase in the control effort, that is acceptable in the cases $\frac{\alpha}{T+\tau}$ equal to 1 and 0.1. The great improvements in the case of $\frac{\alpha}{T+\tau} = 0.01$ are at the cost of a bigger control effort.

Table 5: Numerical example results under random walk disturbance.

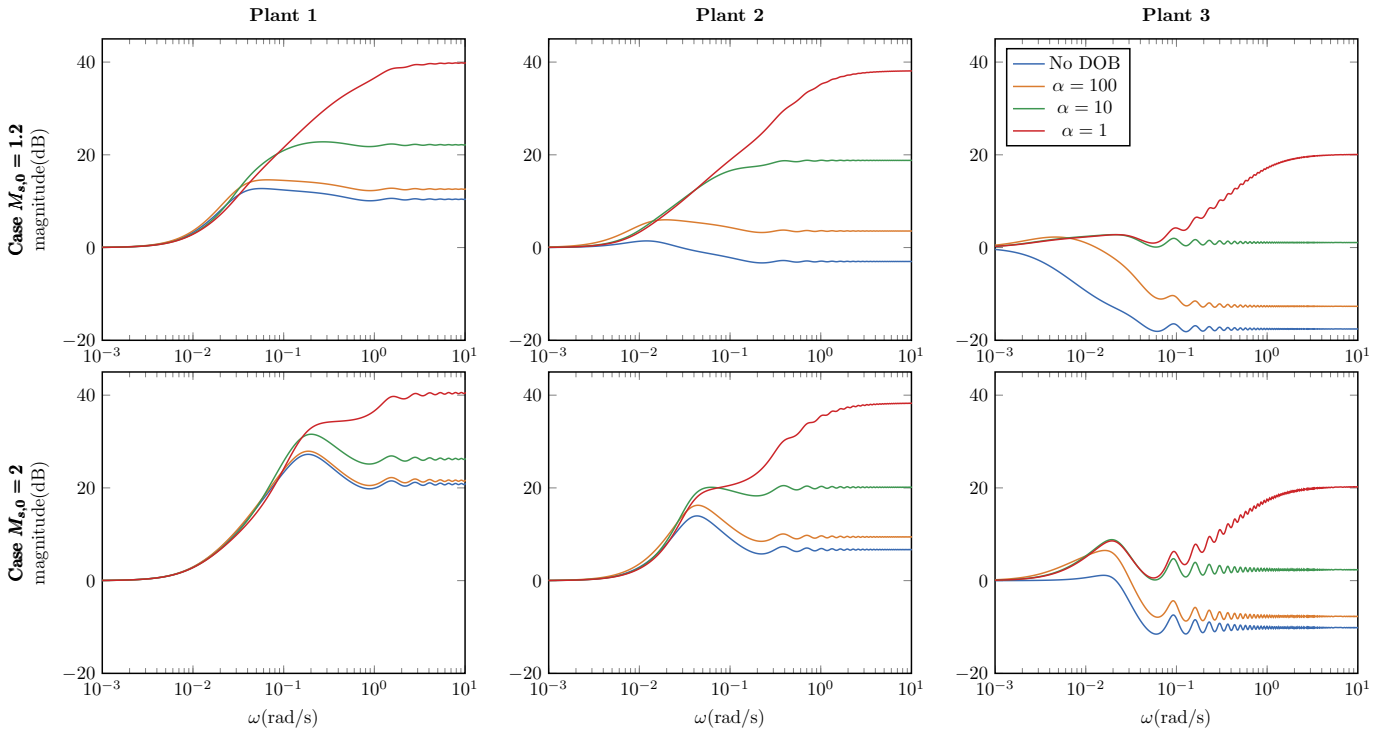

Figure 8: Numerical example. Noise to control action frequency response.

$\frac{\alpha}{T+\tau}$	$\frac{IAE}{IAE_0}$	$\frac{ISE}{ISE_0}$	$\frac{ITAE}{ITAE_0}$	$\frac{e_{\max}}{e_{\max,0}}$	$\frac{TV}{TV_0}$
1	0.9198	0.6894	0.9855	0.6480	1.1858
0.1	0.4202	0.1474	0.4358	0.4028	1.8554
0.01	0.2038	0.0334	0.2008	0.2065	4.1887

5. Trade-off analysis

5.1. FOTD trade-off plots

In this section we extend the analysis of the previous section to all the possible FOTD processes, with normalized time delays in the range $[0, 1]$. We show the effect of process dynamics and the tuning of the parameter α, which we have tested in the range $[0.01, 100]$, on disturbance rejection, robustness and noise amplification.

We compare the behavior of the system including the proposed DOB with the original PI control structure, with its PI tuned to achieve an original sensitivity peak $M_{s,0}$ with the maximum value of K_i. Since the behavior with DOB depends on α, process dynamics and also the original sensitivity peak, three-dimensional trade-offs are required to get full insight. To avoid this, we assume three different values for the original sensitivity peak $M_{s,0}$, covering the reasonable range between 1.2 and 2. All the results in the trade-off plots are relative to the indicators obtained without the DOB. Thus, a value greater than 1 indicates an increase of that indicator when including the DOB, and a value lower than 1, a decrease with respect to the original PI control structure without the DOB.

Figure 10 collects the trade-off plots. The cases analyzed in Section 4 are highlighted with marks. Main conclusions about these figures can be summarized in the following points:

- For the same value of $\alpha/(T + \tau)$, generally the indicators related with performance (IAE, ISE and ITAE) improve more when the PI running on the plant has a lower sensitivity peak $M_{s,0}$ than when the PI presents a higher sensitivity peak.
- The sensitivity peak after including the DOB, M_s, increases as the normalized time delay $T/(T + \tau)$ of the process is higher. This effect is more evident if the PI has a lower sensitivity peak.
- For the same value of $\alpha/(T + \tau)$, noise is amplified more if the PI is tuned with a lower sensitivity peak.
- Good compromises of all the indicators can be achieved when the tuning parameter relative to dynamics, $\alpha/(T+\tau)$, is in the interval [0.01,1]. Two aspects to consider are that we need to be more conservative (not very low values of α) if the normalized time delay is high, because then the sensitivity peak increases more, and that we need to be aware of the measurement noise if we tune α with a very low value.

Generally, in process industry we find PI controllers with very conservative tuning and processes with slow dynamics and low normalized time delay. From previous conclusions, this is the case where the DOB has more advantages because we can achieve better performance and the

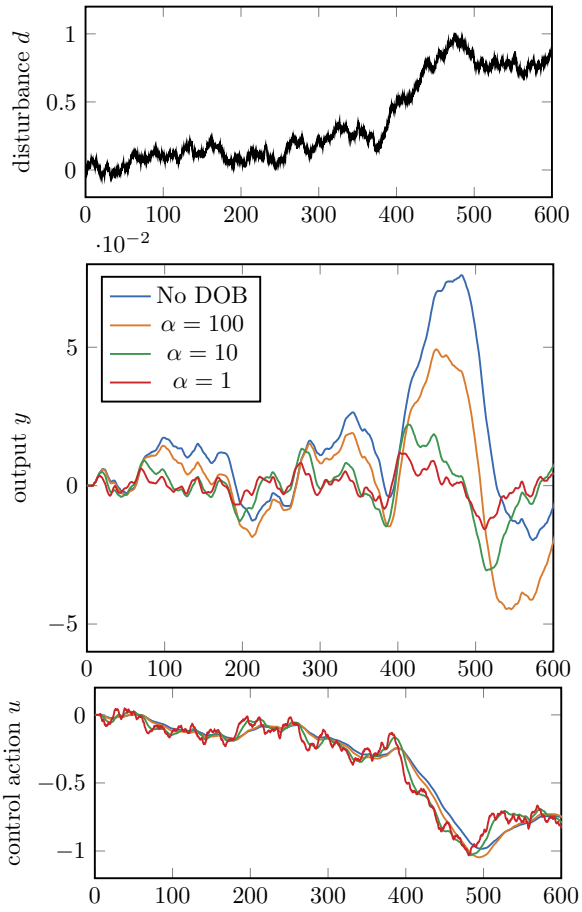

Figure 9: Numerical example. Rejection of a random walk.

sensitivity peak worsening is negligible. This is why we find it suitable to be used in these industries.

5.2. Processes test batch

We have also analyzed the behavior, in terms of the above mentioned indicators, of the proposed DOB applied to the batch of processes proposed in [70], considering representative ones encountered in the process industry. These include integrating, lag-dominant and delay-dominant processes. The complete list of the processes tested is the following:

$$\begin{aligned} P_1(s) &= \frac{e^{-s}}{1+\tau s}, \\ \tau &= 0.02, 0.05, 0.1, 0.2, 0.3, 0.5, 0.7, 1, 1.3, 1.5, \\ &\quad 2, 4, 6, 8, 10, 20, 50, 100, 200, 500, 1000 \end{aligned}$$

$$\begin{aligned} P_2(s) &= \frac{e^{-s}}{(1+\tau s)^2}, \\ \tau &= 0.01, 0.02, 0.05, 0.1, 0.2, 0.3, 0.5, 0.7, 1, 1.3, \\ &\quad 1.5, 2, 4, 6, 8, 10, 20, 50, 100, 200, 500, 1000 \end{aligned}$$

$$\begin{aligned} P_3(s) &= \frac{1}{(1+s)(1+\tau s)^2}, \\ \tau &= 0.005, 0.01, 0.02, 0.05, 0.1, 0.2, 0.5, 2, 5, 10 \end{aligned}$$

$$\begin{aligned} P_4(s) &= \frac{1}{(1+s)^n}, \\ n &= 3, 4, 5, 6, 7, 8 \end{aligned}$$

$$\begin{aligned} P_5(s) &= \frac{1}{(1+s)(1+\tau s)(1+\tau^2 s)(1+\tau^3 s)}, \\ \tau &= 0.1, 0.2, 0.3, 0.4, 0.5, 0.6, 0.7, 0.8, 0.9 \end{aligned}$$

$$\begin{aligned} P_6(s) &= \frac{1}{s(1+s\tau)} e^{-sT}, \tau + T = 1, \\ T &= 0.01, 0.02, 0.05, 0.1, 0.2, 0.3, 0.5, 0.7, 0.9, 1 \end{aligned}$$

$$\begin{aligned} P_7(s) &= \frac{1}{(1+\tau_1 s)(1+\tau_2 s)} e^{-sT}, \tau_2 + T = 1, \\ \tau_1 &= 1, 2, 5, 10 \\ T &= 0.01, 0.02, 0.05, 0.1, 0.3, 0.5, 0.7, 0.9, 1 \end{aligned}$$

$$\begin{aligned} P_8(s) &= \frac{1-\delta s}{(1+s)^3}, \\ \delta &= 0.1, 0.2, 0.3, 0.4, 0.5, 0.6, 0.7, 0.8, 0.9, 1, 1.1 \end{aligned}$$

$$\begin{aligned} P_9(s) &= \frac{1}{(1+s)((\tau s)^2 + 1.4\tau s + 1)}, \\ \tau &= 0.1, 0.2, 0.3, 0.4, 0.5, 0.6, 0.7, 0.8, 0.9 \end{aligned}$$

For each of the 134 processes in the previous list, we have tuned an optimum PI controller by maximizing K_i subject to a sensitivity peak $M_{s,0} = 1.2$. Then, we have tested the step disturbance error response in the system with only the PI controller (getting the indices IAE_0, ISE_0 and $ITAE_0$) and also including the proposed DOB (getting the indices IAE, ISE and $ITAE$). We have tried two different tuning strategies for the DOB parameter α. The first one looks for a noise amplification that is twice the original noise amplification without the DOB ($A_n/A_{n,0} = 2$), which is a more conservative approach in terms of resulting robustness. The second strategy is more aggressive, looking for a noise amplification ten times bigger ($A_n/A_{n,0} = 10$).

Figures 11 and 12 show the ratio between the performance indices obtained with and without the DOB (except M_s, that is an absolute value). A ratio lower than 1 means that the DOB gets better results than the original PI controlled system.

Generally, DOB improves disturbance rejection for any of the previous processes. The only exception is $ITAE$, which can increase if the tuning of the DOB is not aggressive enough ($A_n/A_{n,0} = 2$, which implies higher values of α). As expected, when we use the more aggressive tuning ($A_n/A_{n,0} = 10$), disturbance rejection performance (IAE, ISE, $ITAE$) gets better. As we have seen along the article, higher improvement in disturbance rejection implies a deterioration in robustness and noise amplification.

In summary, in this section we have shown how the proposed DOB, when properly tuned, is suitable for all kind of processes found in industry.

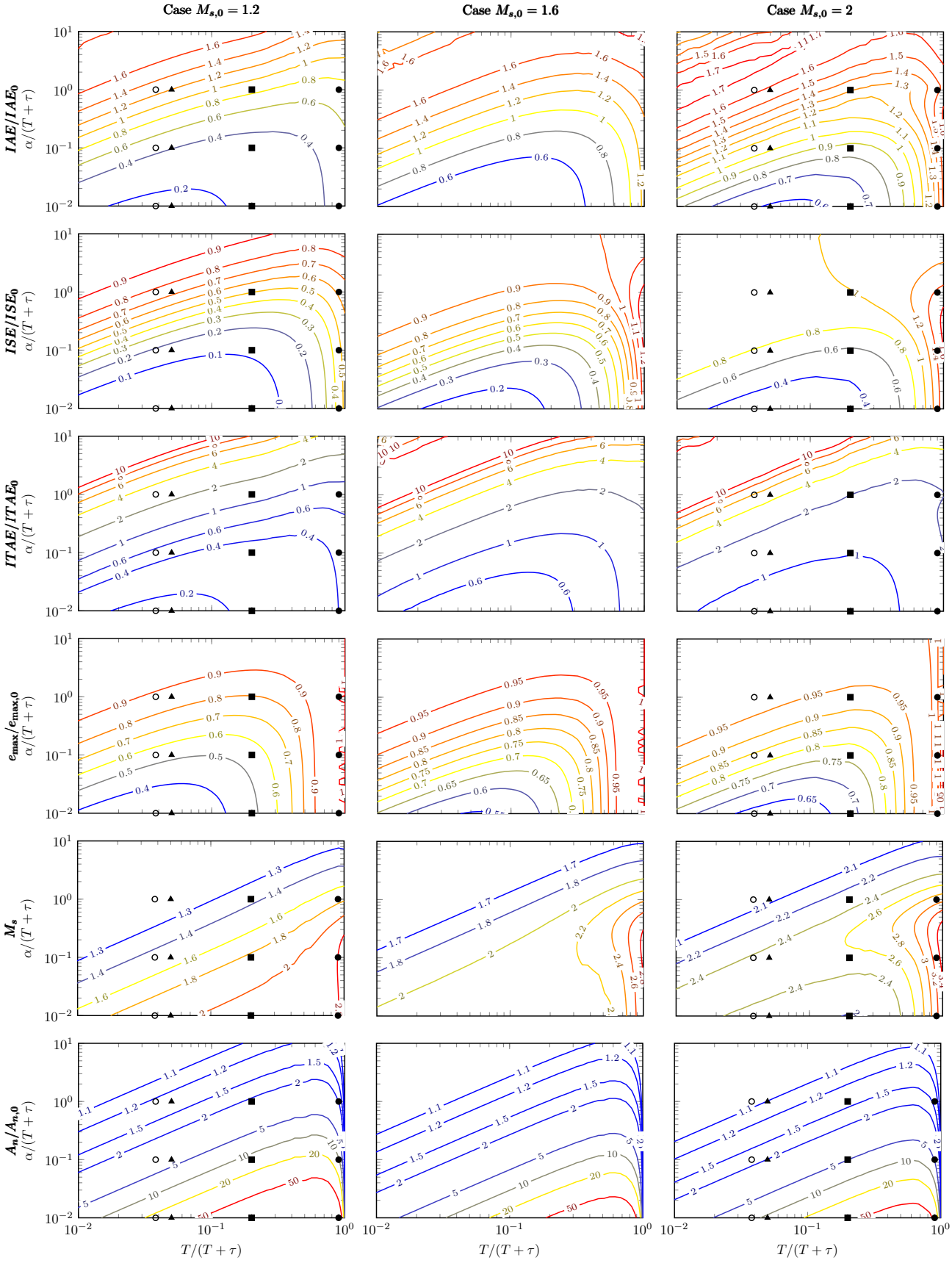

Figure 10: Trade-off plots. Black marks refer to Section 4 examples: ▲ Plant 1, ■ Plant 2, • Plant 3. White mark ○ refers to experimental example in Section 7.

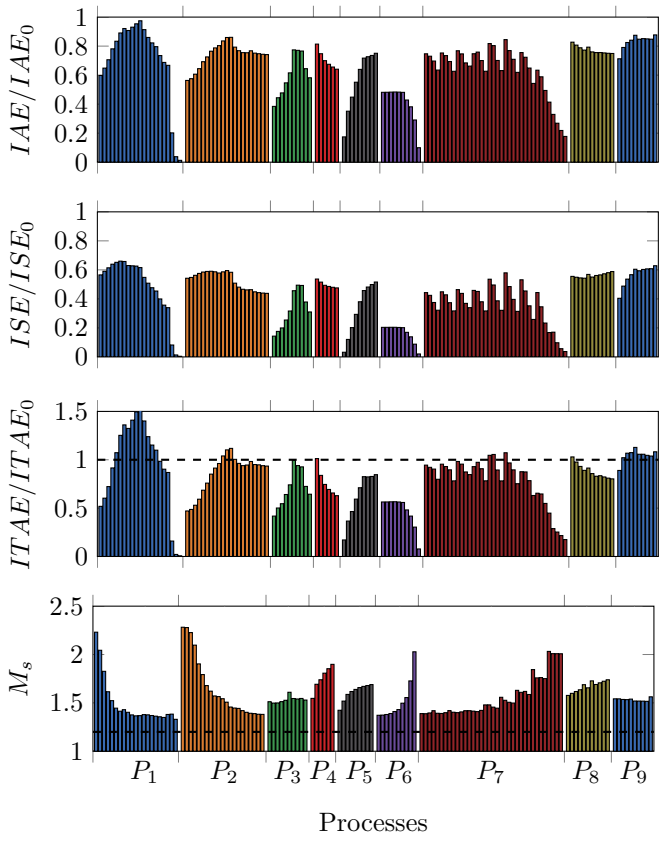

Figure 11: Performance ratio indices for the processes test batch, $A_n/A_{n,0} = 2$.

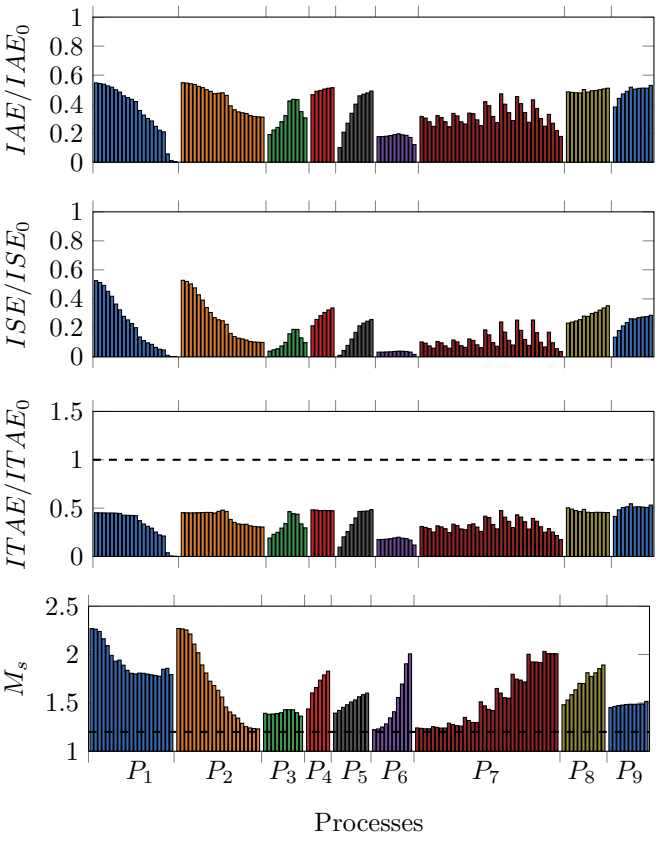

Figure 12: Performance ratio indices for the processes test batch, $A_n/A_{n,0} = 10$.

6. Implementation instructions

This section details the steps to follow for the implementation and proper tuning of the proposed DOB. Our objectives are the following:

- To minimize the disturbance effect.
- To ensure a degree of noise amplification with respect to the initial noise amplification without the DOB,

$$\frac{A_n}{A_{n,0}} \leq b_1. \tag{44}$$

- To ensure a closed loop sensitivity peak (M_s), which will be higher compared with the sensitivity peak without the additive structure ($M_{s,0}$),

$$M_s \leq b_2. \tag{45}$$

For that, we propose these steps:

1. First, we need a process model as (22). Modeling is out of the scope of these work but many methods can be found in the literature.
2. In case the PI controller is not already tuned or running on the plant, we propose an optimal design by maximizing K_i subject to a sensitivity peak in closed loop equal to $M_{s,0}$. Reasonable values of $M_{s,0}$ are in the range $[1.2, 2]$. A higher sensitivity peak gives a more aggressive controller.
3. The design that guarantees the noise amplification b_1 in (36) and (44) is given with the following value for the tuning parameter α:

$$\alpha = \left(\frac{\prod \tau_i}{\prod \beta_i K_p (b_1 - 1)} \right)^{1/d}. \tag{46}$$

Note that for a given process, disturbance rejection with the DOB is better when we let the noise amplification to be higher. This is shown in figure 10 and it is also appreciable if we compare figures 11 and 12.

4. Then, we set C_u and C_y with the structure defined in (26) and (27).
5. Afterwards, we must analyze the closed loop sensitivity peak M_s,

$$M_s = \max_{\omega} |S(j\omega)|,$$

where S is defined in (34). If $M_s > b_2$, we should go back to the step 3 and reduce b_1, iterating until we reach $M_s \leq b_2$.

If we want to tune the parameter α to achieve a desired disturbance rejection performance (as IAE, ISE, ITAE or $e_{\max}$ for step disturbances, or IE for ramp disturbances), the procedure is straightforward: simply start with an arbitrary intermediate value of α, compute the performance, and iterate through α until the desired performance is achieved (reducing α if the performance is not fulfilled, and increasing it if the performance in fulfilled in excess). This procedure is not computationally costly, as the iteration is unidimensional and there is a monotonous inverse relation between performance and α, and can be solved in the tenths of a second in a normal computer.

7. Experimental example

This section presents an example using the proposed DOB with different tunings in a real process, depicted in the figure 13. The system consists of two water tanks. The pump *P-1* boosts water from the feed tank to the other, through a pipeline where the valve *V-1* can regulate the flow. The pump has a driver so we can regulate its speed. The higher tank has a level transducer, *L-1*. There is a drain pipeline with a valve, *V-2*, to return water to the feed tank. At the end of this pipeline there is a connection, *C-1*, which reduces the flow. This has been configured in the laboratory for the test.

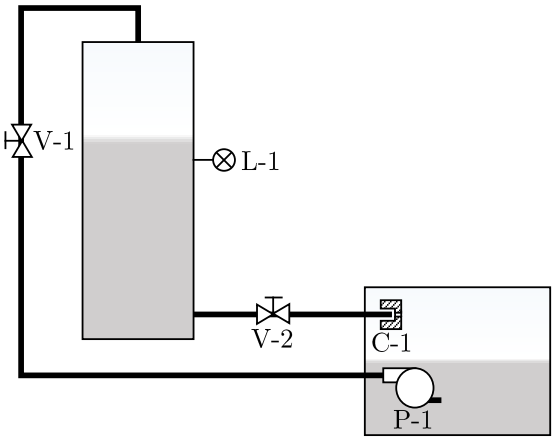

Figure 13: Process for DOB testing

This process is a SISO system where the input u is the duty cycle of the pulse-width modulated signal applied to the DC regulator which drives the pump, in the range $[0, 100]$ %. The applied voltage to the pump is then

$$V_{pump} = \frac{u}{100} V_{cc}, \tag{47}$$

being V_{cc} the voltage of the DC regulator. Initially, that voltage is set to $V_{cc} = 15$ V. The output y is the tank level *L-1*, in the range $[0, 50]$ *cm*. A PI controller is configured to control the tank level y, using u as the control action. Valve *V-1* is initially fully open and the connection *C-1* is properly installed. Valve *V-2* position is used as the disturbance during the test, so we will modify it along the experiment.

First, we have identified the system model, which is

$$G_m(s) = \frac{1.98}{1 + 80.3s} e^{-3.2s}, \tag{48}$$

with time measured in seconds.

With that model, we have tuned two PI controllers maximizing K_i and with sensitivity peaks ($M_{s,0}$) of 1.2 and 2 respectively (C_1 and C_2).

Then, we have also set our DOB with $C_u(s)$ and $C_y(s)$ as

$$C_u(s) = \frac{e^{-3.2s}}{(1 + \alpha\, s)}, \tag{49}$$

$$C_y(s) = -\frac{1 + 80.3\ s}{1.98(1 + \alpha\, s)}. \tag{50}$$

Our process model has a normalized time delay $T/(T + \tau) = 0.038$. Figure 10 can give us insight of the properties of the control system with the DOB in terms of disturbance rejection, robustness and noise amplification, for a given value of α and considering the normalized time delay.

We have tested the system response against step and ramp disturbance types using the two designed PI controllers. The experimented disturbance $d(t)$ (*V-2* valve position) is shown in figure 14. We have repeated the test considering different values for the tuning parameter α: 100%, 10% and 1% of the process $T + \tau$ value. Table 6 summarizes the different experimented configurations.

Table 6: Experimental tests summary

PI	$M_{s,0}$	K_p	T_i
C_1	1.2	2.2	24.6
C_2	2	6.6	10.9

DOB tuning
No DOB, $\alpha = 83.5$, $\alpha = 8.35$, $\alpha = 0.835$.

Figure 14 shows the error response against the experimented disturbance introduced in *V-2* valve position. Figure 15 shows the control action in each case. We can see how disturbance rejection gets more effective as we decrease α. However, this amplifies the noise effect in the control action and reduces the system robustness (the control action has a small oscillatory behavior for lower values of α).

The experimental results show that the behavior is the one expected from the numerical analysis and the trade-off plots. Table 7 show the theoretical result expected according to Figure 10 compared with the measured experimental results. As we expected, a lower value of α in our DOB leads to an improvement in the disturbance rejection, but it implies a higher measurement noise amplification and oscillations in the actuator (i.e., more control effort). The slight differences that one observes in some of the metrics

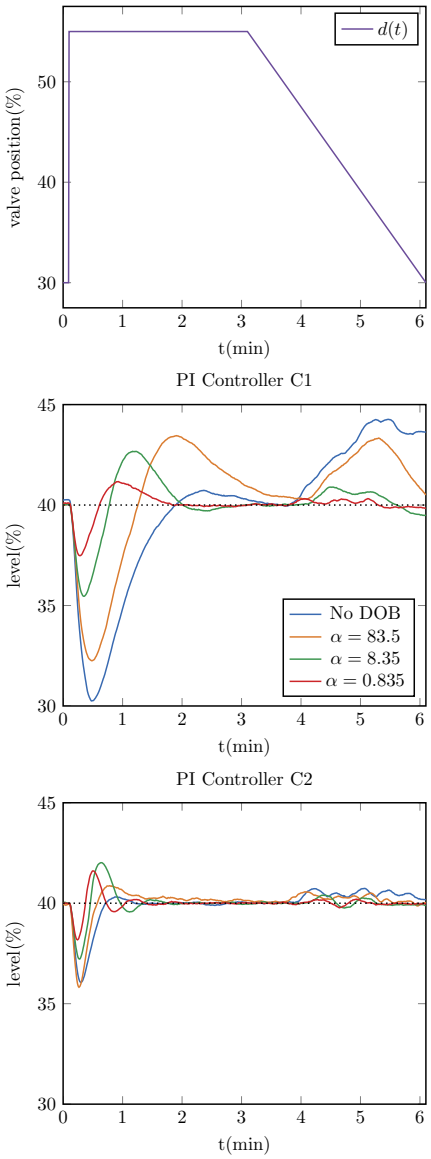

Figure 14: Experimental test. Disturbance effect on the process output.

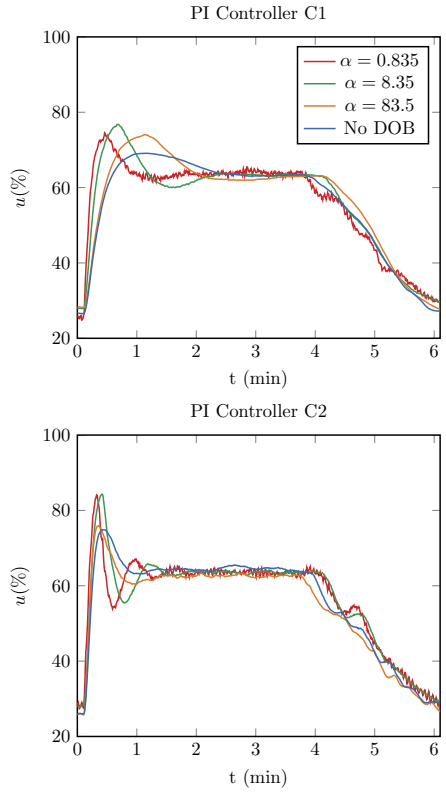

Figure 15: Experimental test. Disturbance effect on the control action.

are due to several factors: the presence of other disturbances in the real process different than the one caused through the valve, the influence of the measurement noise or the duration of the experiment. Furthermore, the theoretical expected metrics are based on a model that can be slightly different from the identified one.

8. Conclusions

In this work, we have presented a Disturbance Observer (DOB) structure appropriate for LTI models, including those with non-minimum phase zeros and time delays (that would make the process inverse unstable or non-realizable). The proposed DOB structure deals with this problem by avoiding the inversion of these elements. We study in detail how the DOB tuning parameter, i.e. the time constant of the DOB filter, affects the closed loop behaviour. For this, we consider as indicators the disturbance rejection performance (IAE, ISE, $ITAE$ and $e_{\max}$), closed loop robustness (sensitivity peak M_s) and noise amplification (the factor compared with the feedback controller noise amplification). Previous indicators present a trade-off, so that a better achievement on one of them implies lower capabilities in the others, which makes DOB tuning not straightforward. In order to give insight about the mentioned trade-off, we have presented trade-off plots for the First Order plus Time Delay (FOTD) case, where we can see how process dynamics and DOB tuning affect those indicators. Furthermore, we have also studied the behaviour of the DOB applied to a benchmark of processes representative in the process industry with two different DOB tuning strategies. We propose simple DOB tuning rules based on this trade-off, as well as instructions for practitioners interested in the implementation. Last, we have tested the DOB structure proposed in a laboratory recreation of a two-tank system, showing experimental results that match the theoretical ones.

One the contributions of the DOB structure proposed in this paper, is that it can be implemented in a plant with an already running PI controller. Other contributions are the simplicity of the DOB tuning rules; its considerations regarding disturbance rejection performance, closed loop robustness and noise amplification, and the detailed study of the mentioned trade-offs.

PI	α	$\frac{IAE}{IAE_0}$		$\frac{ISE}{ISE_0}$		$\frac{ITAE}{ITAE_0}$		$\frac{e_{\max}}{e_{\max,0}}$		$\frac{TV}{TV_0}$
		Theo.	Exp.	Theo.	Exp.	Theo.	Exp.	Theo.	Exp.	Exp.
C_1	83.5	1.297	1.1	0.785	0.728	2.97	1.81	0.886	0.795	1.18
	8.35	0.477	0.444	0.199	0.179	0.557	0.487	0.562	0.466	1.69
	0.835	0.184	0.178	0.039	0.036	0.183	0.16	0.342	0.258	6.04
C_2	83.5	1.682	1.31	0.983	0.963	6.66	2.35	0.976	1.06	1.11
	8.35	1.09	1.00	0.785	0.639	1.46	1.26	0.849	0.71	1.58
	0.835	0.623	0.589	0.32	0.248	0.732	0.71	0.646	0.463	3.99

Table 7: Comparison of theoretical vs experimental results

References

[1] Z. Gao, On the centrality of disturbance rejection in automatic control, ISA Transactions 53 (4) (2014) 850–857.

[2] L. Desborough, R. Miller, Increasing customer value of industrial control performance monitoring-honeywell's experience, in: AIChE symposium series, no. 326, New York; American Institute of Chemical Engineers; 1998, 2002, pp. 169–189.

[3] W. Xue, Y. Huang, Comparison of the DOB based control, a special kind of PID control and ADRC, in: Proceedings of the 2011 American control conference, IEEE, 2011, pp. 4373–4379.

[4] L. Guo, S. Cao, Anti-disturbance control theory for systems with multiple disturbances: A survey, ISA Transactions 53 (4) (2014) 846–849.

[5] D. Chen, D. E. Seborg, PI/PID controller design based on direct synthesis and disturbance rejection, Industrial & Engineering Chemistry Research 41 (19) (2002) 4807–4822.

[6] M. Shamsuzzoha, M. Lee, IMC-PID controller design for improved disturbance rejection of time-delayed processes, Industrial & Engineering Chemistry Research 46 (7) (2007) 2077–2091.

[7] R. Vilanova, O. Arrieta, P. Ponsa, Robust PI/PID controllers for load disturbance based on direct synthesis, ISA Transactions 81 (2018) 177–196.

[8] A. Leva, S. Seva, Structure-specific analytical PID tuning for load disturbance rejection, IFAC-PapersOnLine 51 (4) (2018) 137–142.

[9] R. A. Krohling, J. P. Rey, Design of optimal disturbance rejection PID controllers using genetic algorithms, IEEE Transactions on Evolutionary Computation 5 (1) (2001) 78–82.

[10] R. Garrido, J. L. Luna, On the equivalence between pd+ DOB and PID controllers applied to servo drives, IFAC-PapersOnLine 51 (4) (2018) 95–100.

[11] F. Garcia-Mañas, J. L. Guzmán, F. Rodriguez, M. Berenguel, T. Hägglund, Experimental evaluation of feedforward tuning rules, Control Engineering Practice 114 (2021) 104877.

[12] J. Guzmán, T. Hägglund, Tuning rules for feedforward control from measurable disturbances combined with pid control: a review, International Journal of Control (2021) 1–14.

[13] A. Radke, Z. Gao, A survey of state and disturbance observers for practitioners, in: 2006 American Control Conference, IEEE, 2006, pp. 6–pp.

[14] M. Yuan, C. Manzie, M. Good, I. Shames, L. Gan, F. Keynejad, T. Robinette, A review of industrial tracking control algorithms, Control Engineering Practice 102 (2020) 104536.

[15] K. Ohishi, M. Nakao, K. Ohnishi, K. Miyachi, Microprocessor-controlled dc motor for load-insensitive position servo system, IEEE Transactions on Industrial Electronics 1 (1987) 44–49.

[16] K. Ohishi, T. Miyazaki, Y. Nakamura, High performance ultra-low speed servo system based on doubly coprime factorization and instantaneous speed observer, IEEE/ASME Transactions on Mechatronics 1 (1) (1996) 89–98.

[17] J. Han, From PID to active disturbance rejection control, IEEE Transactions on Industrial Electronics 56 (3) (2009) 900–906.

[18] B. Martinez, J. Sanchis, S. Garcia-Nieto, M. Martinez, Active disturbance rejection control: a guide for design and application, REVISTA IBEROAMERICANA DE AUTOMATICA E INFORMATICA INDUSTRIAL 18 (3) (2021) 201–217.

[19] Y. Xia, B. Liu, M. Fu, Active disturbance rejection control for power plant with a single loop, Asian Journal of Control 14 (1) (2012) 239–250.

[20] Z. Chen, Q. Zheng, Z. Gao, Active disturbance rejection control of chemical processes, in: 2007 IEEE International Conference on Control Applications, IEEE, 2007, pp. 855–861.

[21] L. Sun, D. Li, K. Hu, K. Y. Lee, F. Pan, On tuning and practical implementation of active disturbance rejection controller: a case study from a regenerative heater in a 1000 mw power plant, Industrial & Engineering Chemistry Research 55 (23) (2016) 6686–6695.

[22] L. Sun, Q. Hua, J. Shen, Y. Xue, D. Li, K. Y. Lee, Multi-objective optimization for advanced superheater steam temperature control in a 300 mw power plant, Applied Energy 208 (2017) 592–606.

[23] L. Sun, Y. Jin, F. You, Active disturbance rejection temperature control of open-cathode proton exchange membrane fuel cell, Applied Energy 261 (2020) 114381.

[24] Q. Zheng, Z. Chen, Z. Gao, A practical approach to disturbance decoupling control, Control Engineering Practice 17 (9) (2009) 1016–1025.

[25] L. Sun, J. Dong, D. Li, K. Y. Lee, A practical multivariable control approach based on inverted decoupling and decentralized active disturbance rejection control, Industrial & Engineering Chemistry Research 55 (7) (2016) 2008–2019.

[26] G. Wu, L. Sun, K. Y. Lee, Disturbance rejection control of a fuel cell power plant in a grid-connected system, Control Engineering Practice 60 (2017) 183–192.

[27] C. Fu, W. Tan, Control of unstable processes with time delays via ADRC, ISA Transactions 71 (2017) 530–541.

[28] L. Sun, D. Li, Z. Gao, Z. Yang, S. Zhao, Combined feedforward and model-assisted active disturbance rejection control for non-minimum phase system, ISA Transactions 64 (2016) 24–33.

[29] J.-H. She, M. Fang, Y. Ohyama, H. Hashimoto, M. Wu, Improving disturbance-rejection performance based on an equivalent-input-disturbance approach, IEEE Transactions on Industrial Electronics 55 (1) (2008) 380–389.

[30] Z. Ding, Universal disturbance rejection for nonlinear systems in output feedback form, IEEE Transactions on Automatic Control 48 (7) (2003) 1222–1226.

[31] X. Wei, L. Guo, Composite disturbance-observer-based control and h_∞ control for complex continuous models, International Journal of Robust and Nonlinear Control: IFAC-Affiliated Journal 20 (1) (2010) 106–118.

[32] K. Zhao, J. Zhang, D. Ma, Y. Xia, Composite disturbance rejection attitude control for quadrotor with unknown disturbance, IEEE Transactions on Industrial Electronics 67 (8) (2019) 6894–6903.

[33] Y. Du, W. Cao, J. She, M. Wu, M. Fang, Disturbance rejection via feedforward compensation using an enhanced equivalent-input-disturbance approach, Journal of the Franklin Institute (2020).

[34] S. Kang, R. Nagamune, H. Yan, Almost disturbance decoupling force control for the electro-hydraulic load simulator with mechanical backlash, Mechanical Systems and Signal Processing 135 (2020) 106400.

[35] M. Saków, Novel robust disturbance observer, ISA Transactions (2020).

[36] L. Wang, C. T. Freeman, E. Rogers, Disturbance observer-based predictive repetitive control with constraints, International Journal of Control (2020) 1–10.
[37] J. Teoh, C. Du, G. Guo, L. Xie, Rejecting high frequency disturbances with disturbance observer and phase stabilized control, Mechatronics 18 (1) (2008) 53–60.
[38] X.-S. Chen, J. Li, J. Yang, J.-q. Wang, Disturbance observer enhanced PID decoupling control for multi-variable processes, in: Proceedings of the 32nd Chinese Control Conference, IEEE, 2013, pp. 230–234.
[39] S.-L. Chen, X. Li, C. S. Teo, K. K. Tan, Composite jerk feedforward and disturbance observer for robust tracking of flexible systems, Automatica 80 (2017) 253–260.
[40] Z.-Y. Nie, C. Zhu, Q.-G. Wang, Z. Gao, H. Shao, J.-L. Luo, Design, analysis and application of a new disturbance rejection PID for uncertain systems, ISA Transactions (2020).
[41] Y. I. Son, H. Shim, N. H. Jo, S.-J. Kim, Design of disturbance observer for non-minimum phase systems using PID controllers, in: SICE Annual Conference 2007, IEEE, 2007, pp. 196–201.
[42] Z. Hongdong, Z. Guanghui, S. Huihe, Control of the process with inverse response and dead-time based on disturbance observer, in: Proceedings of the 2005, American Control Conference, 2005., IEEE, 2005, pp. 4826–4831.
[43] J. Yang, S. Li, X. Chen, Q. Li, Disturbance rejection of dead-time processes using disturbance observer and model predictive control, Chemical Engineering Research and Design 89 (2) (2011) 125–135.
[44] Y. A. K. Utama, Y. Hari, Design of PID disturbance observer for temperature control on room heating system, in: 2017 4th International Conference on Electrical Engineering, Computer Science and Informatics (EECSI), IEEE, 2017, pp. 1–6.
[45] J. Carreno-Zagarra, R. Villamizar, J. Moreno, J. Guzmán, Active disturbance rejection and pid control of a one-stage refrigeration cycle, IFAC-PapersOnLine 51 (4) (2018) 444–449.
[46] A. K. Pinagapani, G. Mani, K. Chandran, K. Pandian, Composite disturbance rejection control for ball balancer system, Procedia Computer Science 133 (2018) 124–133.
[47] M.-S. Chen, C.-C. Chen, h_∞ optimal design of robust observer against disturbances, International Journal of Control 87 (6) (2014) 1208–1215.
[48] F. B. Sun, S. W. Zhang, T. W. Zhang, Optimal DOB design for balancing input/output disturbances response, IFAC Proceedings Volumes 47 (3) (2014) 5772–5777.
[49] L. Sun, D. Li, K. Y. Lee, Enhanced decentralized PI control for fluidized bed combustor via advanced disturbance observer, Control Engineering Practice 42 (2015) 128–139.
[50] J. G. Kim, C. H. Han, S. K. Jeong, Disturbance observer-based robust control against model uncertainty and disturbance for a variable speed refrigeration system, International Journal of Refrigeration 116 (2020) 49–58.
[51] L. Wang, J. Cheng, Robust disturbance rejection methodology for unstable non-minimum phase systems via disturbance observer, ISA Transactions 100 (2020) 1–12.
[52] M. Kim, S. Moon, C. Na, D. Lee, Y. Kueon, J. S. Lee, Control of mold level in continuous casting based on a disturbance observer, Journal of Process Control 21 (7) (2011) 1022–1029.
[53] C.-Y. Chen, M.-Y. Cheng, Adaptive disturbance compensation and load torque estimation for speed control of a servomechanism, International Journal of Machine Tools and Manufacture 59 (2012) 6–15.
[54] Y. Xing, J. Na, R. Costa-Castelló, Composite PID control with unknown dynamics estimator for rotomagnet plant, IFAC-PapersOnLine 51 (4) (2018) 817–822.
[55] J. Na, A. S. Chen, G. Herrmann, R. Burke, C. Brace, Vehicle engine torque estimation via unknown input observer and adaptive parameter estimation, IEEE Transactions on Vehicular Technology 67 (1) (2017) 409–422.
[56] X. Du, Q. Jin, Modified disturbance observer-based control for stable multivariate processes with multiple time delays, Journal of Process Control 72 (2018) 52–63.
[57] D. Wang, H. Xiang, Composite control of post-chlorine dosage during drinking water treatment, IEEE Access 7 (2019) 27893–27898.
[58] M.-T. Yan, Y.-J. Shiu, Theory and application of a combined feedback–feedforward control and disturbance observer in linear motor drive wire-edm machines, International Journal of Machine Tools and Manufacture 48 (3-4) (2008) 388–401.
[59] W. Xie, High frequency measurement noise rejection based on disturbance observer, Journal of the Franklin Institute 347 (10) (2010) 1825–1836.
[60] E. Sariyildiz, K. Ohnishi, Analysis the robustness of control systems based on disturbance observer, International Journal of Control 86 (10) (2013) 1733–1743.
[61] J. Han, H. Kim, Y. Joo, N. H. Jo, J. H. Seo, A simple noise reduction disturbance observer and Q-filter design for internal stability, in: 2013 13th International Conference on Control, Automation and Systems (ICCAS 2013), IEEE, 2013, pp. 755–760.
[62] T. He, Z. Wu, Extended disturbance observer with measurement noise reduction for spacecraft attitude stabilization, IEEE Access 7 (2019) 66137–66147.
[63] G. Na, N. H. Jo, Y. Eun, Performance degradation due to measurement noise in control systems with disturbance observers and saturating actuators, Journal of the Franklin Institute 356 (7) (2019) 3922–3947.
[64] O. Garpinger, T. Hägglund, K. J. Åström, Performance and robustness trade-offs in PID control, Journal of Process Control 24 (5) (2014) 568–577.
[65] D. Tena, I. Peñarrocha-Alós, A simple procedure for fault detectors design in siso systems, Control Engineering Practice 96 (2020) 104302.
[66] M. V. Kothare, P. J. Campo, M. Morari, C. N. Nett, A unified framework for the study of anti-windup designs, Automatica 30 (12) (1994) 1869–1883.
[67] Y. Peng, D. Vrancic, R. Hanus, Anti-windup, bumpless, and conditioned transfer techniques for PID controllers, IEEE Control Systems Magazine 16 (4) (1996) 48–57.
[68] S. Skogestad, I. Postlethwaite, Multivariable feedback control: analysis and design, Vol. 2, Wiley New York, 2007.
[69] V. R. Segovia, T. Hägglund, K. J. Åström, Measurement noise filtering for PID controllers, Journal of Process Control 24 (4) (2014) 299–313.
[70] K. J. Åström, T. Hägglund, K. J. Astrom, Advanced PID control, Vol. 461, ISA-The Instrumentation, Systems, and Automation Society Research Triangle, 2006.